**Atmospheric
Measurement
Techniques
Discussions**

Atmospheric Measurement Techniques Discussions is the access reviewed
discussion forum of *Atmospheric Measurement Techniques*

Determination of particulate matter vertical columns using satellite observations

A. A. Kokhanovsky[1], A. S. Prikhach[2], I. L. Katsev[2], and E. P. Zege[2]

[1]Institute of Environmental Physics, O. Hahn Allee, 28334 Bremen, Germany
[2]Institute of Physics, National Academy of Sciences of Belarus, Nezavisimosti Prospekt,
220068, Minsk, Belarus

Correspondence to: A. A. Kokhanovsky (alexk@iup.physik.uni-bremen.de)

AMTD

2, 1027–1055, 2009

**Determination of
particulate matter
vertical columns**

A. A. Kokhanovsky et al.

Title Page

Abstract	Introduction
Conclusions	References
Tables	Figures

|◄ | ►|

◄ | ►

Back | Close

Full Screen / Esc

Printer-friendly Version

Interactive Discussion

Abstract

A new technique to retrieve the particulate matter vertical columns from spaceborne observations is described. The method is based on the measurements of the spectral aerosol optical thickness (AOT). The spectral slope of the derived aerosol optical thickness is used to infer the size of particles, which is needed (along with the absolute value of AOT) to determine corresponding vertical columns. The technique is applied to the case of a cloudless atmosphere over Germany and results are compared with ground-based observations.

1 Introduction

Atmospheric gases (e.g., O_3, SO_2, NO_2) and particles suspended in atmosphere are known to contribute to the increased mortality in areas with high concentrations of corresponding pollutants (Altshuller, 1972; Pope et al., 2002). Therefore, there is an urgent task to monitor and reduce levels of pollution. The corresponding ground-based observation systems are in place in a number of national environmental agencies. Most of these systems do not include satellite observations at the moment. Browse imagery of cloud fields is known to everybody due to weather forecasts broadcasted on TV. Similar forecasts must be developed for the gaseous and particulate matter pollution monitoring based on space-borne observations from a geostationary orbit. Snapshots derived using polar orbiting instruments are of importance as well.

The top-of-atmosphere (TOA) reflectance measured by an optical instrument on a satellite platform is determined not only by the underlying surface reflectance of solar light (e.g., snow, ice, sand, vegetation) but also by vertical distributions of microphysical characteristics of particles and gases suspended in atmosphere. Therefore, there is a possibility to derive vertical columns of gases and also suspended particles from passive spectral top-of-atmosphere solar light reflectance measurements. This subject is actively explored at the moment in a number of national and international agencies

Title Page

Abstract | Introduction

Conclusions | References

Tables | Figures

|◀ | ▶|

◀ | ▶

Back | Close

Full Screen / Esc

Printer-friendly Version

Interactive Discussion

and research organizations (Burrows, 1999; Borell et al., 2004; Al-Saadi et al., 2005). The task of this paper is to introduce a novel technique for the determination of particulate matter vertical concentration from space. The size of particles needed in the calculation of the aerosol mass is derived from the retrieved spectral aerosol optical thickness.

The paper is structured as follows. In the next section we present the methodology of particulate matter vertical columns (PMVC) retrievals from space developed by us. The Sect. 3 is aimed at the applications and the validation of the developed technique using ground – based measurements. Outlook and conclusions are discussed in the final section of the paper.

2 Methodology

The retrieval of aerosol mass concentration using space-borne observations has been performed by several groups (see, e.g., Griggs, 1975, 1979; Fraser, 1976; Fraser et al., 1984; Kaufman and Fraser, 1990; Gasso and Hegg, 1997; 2003). They are based on the fact that the aerosol number concentration per unit area $n=NL$ (for the beginning let us consider a homogeneous layer, N is the number concentration of particles (cm^{-3}), L is the geometrical thickness of this layer) can be related to the aerosol optical thickness (AOT) τ routinely measured by satellites both over land and ocean (see, e.g., Remer et al., 2005; Kokhanovsky and de Leeuw, 2009). Namely it follows:

$$n = A\tau, \tag{1}$$

where the constant A depends on the particle size distribution, the chemical composition and the shape of particles. It is often assumed for the simplification of the particulate matter (PM) retrievals that the tropospheric aerosol is mostly contained in a lower atmospheric boundary layer (with the thickness L of 1 km or so) and well mixed there.

Then it follows for a homogeneous aerosol layer:

$$A = \frac{1}{C_{ext}}, \tag{2}$$

where C_{ext} is the average extinction cross section of particles in a mixing layer. The value of L can be measured, e.g., with a lidar. Then the concentration N can be also estimated.

The aerosol mass concentration m per unit area (g/cm^2) can be found from the following equation:

$$m = nV\rho, \tag{3}$$

where V is the average volume of particles and ρ is the average density of aerosol particles assumed to be equal 1 g/cm^3 in this work. Therefore, the final equation reads (see Eqs. 1, 2):

$$m = \frac{V\rho\tau}{C_{ext}}, \tag{4}$$

or, introducing the effective optical size of particles (OSP)

$$a = V/C_{ext}, \tag{5}$$

one derives:

$$m = a\rho\tau. \tag{6}$$

It follows in the case of a homogeneous layer for the aerosol mass concentration (g/cm^3): $M = m/L$. Therefore, the mass concentration M correlates with the product $a\rho\tau L^{-1}$ rather than with τ itself. This in part explains the differences between seasonal patterns of AOT as compared to the ground-measured PM seasonal variations described by Xia et al. (2006). Other reason for such differences could be the aerosol vertical distribution (e.g., decoupling of aerosol layers with a heavy load of particles

Determination of particulate matter vertical columns

A. A. Kokhanovsky et al.

Title Page

Abstract | Introduction

Conclusions | References

Tables | Figures

◄ | ►

◄ | ►

Back | Close

Full Screen / Esc

Printer-friendly Version

Interactive Discussion

from the atmospheric boundary layer). Strong correlations between PM and τ as described, e.g., by Al-Saadi et al. (2005) should be taken with caution (at least as far as the universal nature of these correlations is of concern).

The OSP (or scaling constant) a should be studied depending on air masses, season, and locations. Also theoretical calculations of this parameter could be performed. For instance, it follows for large (the size is much larger than the wavelength λ) convex randomly oriented particles (van de Hulst, 1981): $C_{ext}=S/2$, where S is the average surface area of particles. This result does not depend on the shape and also on the chemical composition of particles providing that the size of particles is much larger than the wavelength and the refractive index is not close to unity. These conditions hold for the desert dust outbreaks. Then it follows:

$$a = \frac{2a_{ef}}{3},\qquad(7)$$

where $a_{ef}=3V/S$ is the effective radius (ER) of particles. Estimations of ER enable the determination of PMVC for dust outbreaks from the retrieved AOT (see Eq. 6). This is of importance, e.g., for calculations of particulate mass fluxes from deserts to oceans (Gasso and Hegg, 2003; Desboeufs and Cautenet, 2005).

The size of atmospheric particles in most of cases is smaller than the wavelength of the visible light. The typical effective radii are of about 100 nm. Therefore, the approach for the calculation of the OSP a for large particles given above can not be followed in most of cases. The retrieval of PMVC from space is possible, only if the correspondent model for the derivation of OSP is established. We propose the following route to estimate PMVC from satellite measurements:

– The aerosol optical thickness at several wavelengths λ is determined from satellite measurements.

– The Angstrom coefficient α is determined as the slope of $\ln \tau (\lambda)$.

A. A. Kokhanovsky et al.

– The following analytical relationship between a_{ef} and α is used:

$$a_{ef} = 10^p \ (\mu m) , \ \text{where } p = \sum_{n=0}^{4} A_n \alpha^n ,$$

$A_0 = -0.07075, A_1 = -1.03109, A_2 = 0.72806, A_3 = -0.41111, A_4 = 0.08106.$

The constants A_j were derived using the calculation of extinction coefficients with the Mie theory at the refractive index 1.45+0.005i and λ=412 and 670 nm. The lognormal size distribution with the standard deviation equal to the average size of particles is used (the lognormal size distribution with the width parameter σ=0.8326, Kokhanovsky et al., 2006).

– The value of C_{ext} is found from the parameterization of Mie calculations for the same size distribution as above using the derived value of a_{ef} and assuming the complex refractive index of particles 1.45+0.005i. In particular, the following relationship is used (Kokhanovsky et al., 2006):

$$C_{\text{ext}} = \pi a_{ef}^2 \exp\left(-3\sigma^2\right) Q_{\text{ext}}, \qquad \lg(Q_{\text{ext}}) = \sum_{n=0}^{4} B_n \lg^n (k a_{ef}) , \tag{8}$$

where

σ=0.8326, k=2π/λ, $B_0 = -0.367, B_1 = 1.76, B_2 = -1.024, B_3 = -0.095, B_4 = 0.143.$

– The PMVC is found from Eq. (4), where the average volume V is calculated from the derived a_{ef} assuming the single mode lognormal distribution with the half-width equal to the average radius as proposed by Kokhanovsky et al. (2006). Namely, it follows: $V \approx \pi a_{ef}^3/6$ at σ=0.8326. The value of L can be found from lidar measurements or European Centre for Medium-Range Weather Forecasting

(ECMWF) analysis. If the value of L is known, then $PM_{10} = PMVC/L$ can be also determined.

As seen the proposed technique has advantages over the methods relying on *a priori* assumed values of OSP. The drawbacks of the model are the assumption of the fixed single mode particle size distribution and the refractive index of particles. They can be overcome in future, if the multi-angle space Stokes polarimeters will be launched (Mishchenko et al., 2005). This will bring a wealth of necessary information, which is not available in the spectral top-of-atmosphere measurements used in this paper and would allow to avoid some assumptions used in the technique described above. Therefore, several assumptions have been made to retrieve PMVC in this paper.

Now let us use the proposed technique to estimate PMVC from satellite data.

The algorithm for the determination of the aerosol optical thickness over land applied in this study (Katsev et al., 2009) will be reviewed in the next section. The PM retrieval technique as given above can be used in conjunction with any existing aerosol retrieval algorithm for the determination of $\tau(\lambda)$ over land or ocean. The correct determination of α is crucial for the performance of the algorithm.

3 Retrievals and their validation

3.1 Aerosol optical thickness

The spectral optical thickness and Angstrom parameter has been derived using the Aerosol Retrieval Technique (ART) developed by Katsev et al. (2009). The algorithm is based on the iterative solution of the vector radiative transfer equation. Retrievals in this paper are performed using standard continental aerosol model (WMO, 1986) (see Fig. 1). According to this model, the single scattering albedo is equal to 0.9 at the wavelength $\lambda=550$ nm. Over land, two *a priori* ground reflectance spectra are assumed (for the bare soil ($r_s(\lambda)$)) and for the vegetated surface ($r_v(\lambda)$), see Fig. 2) in our retrieval

procedure. The corresponding spectra were derived using measurements from a low altitude aircraft (von Hoyningen – Huene et al., 2003, 2006).

It is taken that a linear combination of these basic spectra with mixture parameter c describes the ground reflectance spectra:

$$r(\lambda) = cr_v(\lambda) + (1 - c)r_s(\lambda) \tag{9}$$

The parameters $\tau_* \equiv \tau\,(412\,\text{nm})$, α and c do not depend on the wavelength by definition. They are derived from the measured spectral TOA reflectance with use of the least square technique by the iteration process.

We have selected the MEdium Resolution Imaging Spectrometer (MERIS) on board ENVIronmental SATellite (ENVISAT) data over Germany for 13 October 2005 for the validation of our technique. Clouds were almost absent at that day over most of Germany (Kokhanovsky et al., 2008). Full resolution MERIS scenes have the spatial resolution 260m across track and 290 m along track. The reduced resolution mode used in this work has a spatial resolution 1040 m across track and 1160 m along track. Full resolution full scene has 2241×2241 pixels and covers 582 km (swath) by 650 km (azimuth). Reduced resolution scenes have 1121×1121 pixels and cover 1165 km (swath) by 1300 km (azimuth). MERIS performes measurements at the wavelengths 412.5 nm, 442.5 nm, 490 nm, 510 nm, 560 nm, 620 nm, 665 nm, 681.3 nm, 708.8 nm, 753.8 nm, 760.6 nm, 778.8 nm, 865 nm, 885 nm, 900 nm. The channels at 670 and 865 nm have been used for the determination of Normalized Difference Vegetation Index (NDVI=$(R(\lambda_2) - R(\lambda_1))/(R(\lambda_2) + R(\lambda_1)$, λ_1=670 nm, λ_2=865 nm) from the spectral reflectance $R(\lambda)$ measurements. NDVI is used as an initial guess value for c. All used channels have the bandwidth of 10 nm (except the channel at 865, which has the bandwidth of 20 nm). Further details on the MERIS and its measurement modes are given by Bezy et al. (2000).

The correlation plot of the ART-retrieved AOT and ground-based AERONET measurements of τ (Holben et al., 1998) is shown in Fig. 3 at the AERONET wavelengths 440 nm and 670 nm. Generally, the agreement is good.

The summary of results for 9 AERONET stations is shown in Tables 1 and 2. Figure 4 gives the difference Δ=AOT (satellite)-AOT (AERONET) for both wavelengths as the function of AERONET-measured AOT. One can see that ART performs quite well for all AERONET sites. Absolute differences in the retrieved and AERONET-measured τ are

5 smaller than 0.06 for most of cases at both wavelengths, which is a promising result. Some differences can be explained by the fact that the satellite-derived AOT is for $5\times5\,km^2$ grid box over the AERONET site. Therefore, it can be influenced by the local distribution of pollution not seen by AERONET point measurements and vice versa. As it follows from Table 2, the average values of ground and satellite-derived AOTs

10 are very close. We conclude that the aerosol optical thickness is determined quite accurately for both channels and is within MODIS AOT estimation error $\pm0.05\pm0.15\tau$ (Levy, 2009) for most of cases (see Fig. 4).

The retrieved Angstrom parameter α is given in Table 3 and in Fig. 5. These results show that ART also makes accurate estimates of α. The average value of α for all

15 AERONET stations is 1.45 and it is 1.41 for satellite observations. It follows that the absolute values of differences between values of α derived from satellite and ground observations $\Delta=\alpha^s-\alpha^a$ do not exceed 0.3.

The spatial distributions of aerosol optical thickness at 412 nm and the Angstrom exponent for almost cloud free scene over Germany and neighboring countries are

20 given in Figs. 6, 7, respectively. We see that the Angstrom coefficient does not vary considerably over the scene being around 1.3, which is close to average value for the atmospheric conditions in Germany. Although we see a considerable variability in the retrieved AOT with larger values in the northern Germany.

3.2 Particulate matter vertical columns

25 The derived values of AOT and α were used to determine the particulate matter vertical columns. This was done according to the procedure described in the previous section. First of all, the effective radius (see Fig. 8) and the values of V and C_{ext} were assessed. Then PMVC is calculated using Eq. (4). The corresponding maps are presented in

Figs. 8, 9 for a_{ef} and m, respectively. The value of α (and a_{ef}) does not vary much along the scene. Therefore, the PMVC pattern shown in Fig. 9 is similar to that of AOT (but not identical).

The following features can be derived from this map:

5 – the increased level of pollution in the Frankfurt and Berlin areas;

– clear air north of Alps and in the south-western Germany (Freiburg);

– clear air in the Northwestern Germany and eastern part of Belgium;

– pollution around Amsterdam.

Overall, it appears that the analysis of PMVC maps could be of benefit for national and also international environmental agencies, especially as far as the studies of the trans-boundary pollution transfer is of concern (see, e.g., the area east of Berlin).

It is difficult to validate the derived PMVC. This is because of several circumstances:

1. The retrieved values represent the average numbers for the whole atmospheric vertical column; the measurements of PM at the ground are representative for local measurement points only.

2. The results of ground measurements can vary spatially inside of one MERIS pixel (e.g., close to the road and 1 km from the road). Therefore, for the correct comparisons, ground measurements must be performed not at one place but in several places in the pixel.

3. AOTs measured from ground and space represent the same physical quantity, namely, the aerosol extinction coefficient integrated along the vertical path. This is not the case for the satellite and ground – derived PM. Indeed, the satellite-derived PMVC represents the whole atmospheric column from the ground to the TOA. Ground measurements are performed at the height h=2 m above the ground

Determination of particulate matter vertical columns

A. A. Kokhanovsky et al.

level. Also the weighting methods are used to determine the aerosol mass. There-fore, mostly dry fraction of aerosol is measured and not the ambient aerosol as it is done for the satellite measurements. Although indeed attempts can be made to correlate ground measured PM with M=m/L, where the aerosol layer thick-ness L must be assessed using, e.g., lidar measurements (Kokhanovsky et al., 2006). The boundary layer height as derived from ECMWF analysis has some uncertainty, which contributes to the discrepancy of satellite and ground mea-surements.

4. The aerosol layer can be decoupled from the surface. Then the satellite signal is influenced mostly by the aerosol in this layer and, therefore, the contribution of light interacted with the aerosol at the ground level to the satellite measurements is negligible and can not be assessed.

These and some other factors lead to the fact that the satellite-derived and ground-measured PM poorly correlate. Poor correlation is also seen in our Fig. 10, where we correlate PM_{10} (PM with diameters of particles smaller than $10\,\mu$m) with MERIS PM M=m/L measurements, where L is the boundary layer height taken from the ECMWF analysis.

The part of poor correlation can be explained by the fact that the spatial distribu-tion of used satellite imagery is not capable to detect small scale perturbations of PM detectable using ground measurements (see the results with large PM values (traffic) presented in Fig. 11). However, this does not mean that satellite measurements are useless with respect to particulate matter pollution monitoring. They just bring addi-tional type of information as shown in Fig. 9. Also we found that average values are close for ground and satellite measurements. For the cases shown in Fig. 10, the average ground PM_{10} is $50\,\mu$g/m^3 and it is just by $4\,\mu$g/m^3 smaller for the satellite retrievals (see Fig. 11 as well). More importantly, ground measurements of PM in dif-ferent countries differ – so if you put two instruments at the same place, they often do not produce the same results for PM_{10} due to differences in instruments and software.

Determination of particulate matter vertical columns

A. A. Kokhanovsky et al.

Satellite measurements have a shortcoming that they are related not to point measurements but to vertical columns. So information is not resolved with respect to vertical and horizontal coordinates. It is also not resolved with respect to time because (if the measurements are performed not from a geostationary orbit) the measurements only once per day are possible (e.g., morning around 10:00 local time for ENVISAT). Even a small subpixel cloud or snow fraction of 10% or so destroys all retrievals completely. This reduces the capabilities of satellite methods to observe PMVC even further.

The superiority of satellite data is in their low cost, global processing (for any place on the planet) and the possibility to assess the pollution levels over a large area. In particular, ground measurements are not capable to cover the whole country with 1 km – scale network but this is easy done with satellite measurements as demonstrated in Fig. 9. Also satellite data can be used for processing long term data of the same quality and using the same algorithm. This helps to identify trends relevant for environmental and climatic studies.

4   Conclusions

We have proposed a technique to determine the particulate matter vertical columns from space-based observations. The technique was compared with ground measurements of PM_{10} in Germany. Results obtained are encouraging. The spaceborne observations can not substitute ground-based measurements due to problems with the technique for cloudy and bright underlying surface (e.g., snow) scenes, etc. However, they can be used to enhance the accuracy of interpolation between single point retrievals as performed by the ground network nowadays. They can be used also for the improvement of aerosol global modeling. The derived values of a_{ef} are of importance for the estimations of surfaces available for atmospheric heterogeneous reactions. The maps as shown in Fig. 9 can be utilized by environmental agencies in their daily work in future. An interesting point not considered in this work is the determination of $PM_{2.5}$ from space. Namely these small particles with sizes below 2.5 μm are of major importance

as far as health issues are of concern. One way to determine PM$_{2.5}$ concentration is to use correlations between PM$_{2.5}$ and derived PM$_{10}$ valid for a particular location.

References

Al-Saadi, J., Szykman, J., Pierce, R. B., et al.: Improvings national air quality forecasts with satellite aerosol observations, B. Am. Meteorol. Soc., 9, 1249–1261, 2005.

Altshuller, A. P.: Atmospheric sulfur dioxide and sulfate: distribution of concentrations at urban and non-urban sites in the United States, Environ. Sci. Technol., 7, 709–712, 1973.

Bezy, J.-L., Delwart, S., and Rast, M.: MERIS – a new generation of ocean colour sensor onboard ENVISAT, ESA Bulletin, 103, 48–6, 2000.

Borell, P., Borell, P. M., Burrows, J. P., and Platt, U. (eds.): Sounding the troposphere from space: a new era of atmospheric chemistry, Springer-Verlag, Berlin, Germany, 2004.

Burrows, J. P.: Current and future passive remote sensing techniques used to determine atmospheric constituents, Approaches to Scaling o f Trace Gas Fluxes in Ecosystems, edited by: Bouwman, A. F., Elsevier, Dordrecht, The Netherlands, 317–347, 1999.

Desboeufs, K. V. and Cautenet, G.: Transport and mixing zone of desert dust and sulphate over Tropical Africa and the Atlantic Ocean region, Atmos. Chem. Phys. Discuss., 5, 5615–5644, 2005,
http://www.atmos-chem-phys-discuss.net/5/5615/2005/.

Fraser, R. S.: Satellite measurement of mass of Sahara dust in the atmosphere, Appl. Optics, 15, 2471–2479, 1976.

Fraser, R. S., Kaufman, Y. J., and Mahoney, R. L.: Satellite measurements of aerosol mass and transport, Atmos. Environ., 18, 2577–2584, 1984.

Gasso , S. and Hegg, D. A.: Comparison of columnar aerosol optical properties measured

by the MODIS airborne simulator with in situ measurements: A case study, Remote Sens. Environ., 66, 138–152, 1997.

Gasso, S. and Hegg, D. A.: On the retrieval of columnar aerosol mass and CCN concentration by MODIS, J. Geophys. Res., 108(D1), 4010, doi:10.1029/2002JD002382, 2003.

5 Griggs, M.: Measurements of atmospheric aerosols over water using ERTS-1 data, Air Pollution Control Association Journal, 25, 622–626, 1975.

Griggs, M.: Satellite observations of atmospheric aerosols during the EOMET cruise, J. Atmos. Sci., 36, 695–698, 1979.

Hanel, G.: The properties of atmospheric aerosol particles as a function of relative humidity at
10 thermodynamic equilibrium with surrounding moist air, Adv. Geophys., 19, 73–188, 1976.

Holben, B. N., Eck, T. F., Slutsker, I., et al.: AERONET – a federated instrument network and data archive for aerosol characterization, Remote Sens. Environ., 66, 1–16, 1998.

Katsev, I. L., Prikhach, A. S., Zege, E. P., Ivanov, A. P., and Kokhanovsky, A. A.: Iterative procedure for retrieval of spectral aerosol optical thickness and surface reflecatnce from satellite
15 data using fast radiative transfer code and its application to MERIS onboard ENVISAT measurements, in: Satellite Aerosol Remote Sensing over Land, edited by: Kokhanovsky, A. A. and de Leeuw, G., Springer-Praxis, Berlin, Germany, 101–134, 2009.

Kaufman, Y. J. and Fraser, R. S.: Satellite measurements of large-scale air pollution: Methods, J. Geophys. Res., D95, 9895–9909, 1990.

20 Kokhanovsky, A. A., von Hoyningen-Huene, W., and Burrows, J. P.: Atmospheric aerosol load as derived from space, Atmos. Res., 81, 176–185, 2006.

Kokhanovsky, A. A.: Aerosol Optics, Praxis-Springer, Berlin, 2008.

Kokhanovsky, A. A. and de Leeuw, G. (eds.): Satellite Aerosol Remote Sensing over Land, Springer-Praxis, Berlin, 2009.

25 Levy, R. C.: The dark-land MODIS collection 5 aerosol retrieval: algorithm development and product evaluation, in: Satellite Aerosol Remote Sensing over Land, edited by: Kokhanovsky, A. A. and de Leeuw, G., Springer-Praxis, Berlin, 19–68, 2009.

Liou, K. N.: Introduction to Atmospheric Radiation, Academic Press, NY, USA, 2002.

Mishchenko, M. I., Cairns, B., Chowdhary, J., et al.: Remote sensing of terrestrial tropospheric
30 aerosols from aircraft and satellites, J. Phys. Conference Series, 6, 73–89, 2005.

Pope, C. A., Burnett, R. T., Thun, M. J., et al.: Lung cancer, cardiopulmonary mortality and long-term exposure to fine particulate air pollution, Journal of American Medical Association, 287, 1132–1141, 2002.

Remer, L. A., Kaufman, Y. J., Tanré, D., et al.: The MODIS Aerosol Algorithm, Products and Validation, J. Atmos. Sci., 62, 947–973, 2005.

Tomasi, C., Vitale, V., Petkov, B., et al.: Improved algorithm for calculations of Rayleigh-scattering optical depth in standard atmospheres, Appl. Optics, 44, 3320–3341, 2005.

van de Hulst, H. C.: Light Scattering by Small Particles, Dover, NY, USA, 1981.

von Hoyningen-Huene, W., Freitag, M., and Burrows, J. P.: Retrieval of aerosol optical thickness over land surfaces from top-of-atmosphere radiance, J. Geophys. Res., 108(D9), 4260, doi:10.1029/2001JD002018, 2003.

von Hoyningen-Huene, W., Kokhanovsky, A. A., Burrows, J. P., et al.: Simultaneous determination of aerosol and surface characteristics from top-of-atmosphere reflectance using MERIS on board of ENVISAT, Advances in Space Research, 37, 2172–2177, 2006.

WMO: International Association for Meteorology and Atmospheric Physics Radiation Commission: A preliminary cloudless standard atmosphere for radiation computation, World Climate Program, WCP-112, WMO TD-24, World Meteorological Organisation, Geneva, Switzerland, 1986.

Xia, X. A., Chen, H. B., Wang, P. C., et al.: Variation of column-integrated aerosol properties in a Chinese urban region, J. Geophys. Res., 111, D05204, doi:10.1029/2005JD006203, 2006.

Table 1. The AERONET τ^a and satellite τ^s retrieved values of the aerosol optical thickness for 13 September 2005 (10:00 UTC).

Station	Position	Time	τ^a_{440}	τ^s_{440}	Δ_{440}	τ^a_{670}	τ^s_{670}	Δ_{670}
Hamburg	53.568 N, 9.973 E	09:52	0.21	0.27	−0.06	0.11	0.15	−0.04
Helgoland	54.178 N, 7.887 E	09:45	0.27	0.33	−0.06	0.15	0.17	−0.02
Cabauw	51.971 N, 4.927 E	09:57	0.25	0.25	0.00	0.15	0.13	0.02
Den Haag	52.110 N, 4.327 E	09:44	0.31	0.43	−0.12	0.16	0.24	−0.08
Leipzig	51.354 N, 12.435 E	10:06	0.24	0.26	−0.02	0.13	0.15	−0.02
Mainz	49.999 N, 8.300 E	09:58	0.42	0.31	0.11	0.24	0.17	0.07
Karsruhe	49.093 N, 8.428 E	09:43	0.31	0.28	0.03	0.16	0.16	0.00
Venice	45.314 N, 12.508 E	09:29	0.47	0.63	−0.16	0.24	0.34	−0.10
Bremen[*]	53.05 N, 8.78 E	10:06	0.35	0.29	0.06	0.2	0.17	0.03

[*] not in AERONET.

Table 2. The difference between AERONET and satellite measurements of AOT (averaged for all stations).

λ, nm	$\bar{\tau}^a$	$\bar{\tau}^s$	$\Delta\tau$
440	0.31	0.34	0.03
670	0.17	0.19	−0.02

Determination of particulate matter vertical columns

A. A. Kokhanovsky et al.

Table 3. Angstrom components and corresponding relative differences δ.

Station	α_g	α_s	δ, %
Hamburg	1.54	1.44	6.49
Helgoland	1.4	1.54	−10.00
Cabauw	1.21	1.43	−18.18
Den Haag	1.57	1.41	10.19
Leipzig	1.46	1.36	6.85
Mainz	1.33	1.41	−6.02
Karsruhe	1.57	1.36	13.38
Venice	1.6	1.46	8.75
Bremen	1.33	1.32	0.75

Title Page

Abstract | Introduction

Conclusions | References

Tables | Figures

◄◄ | ►►

◄ | ►

Back | Close

Full Screen / Esc

Printer-friendly Version

Interactive Discussion
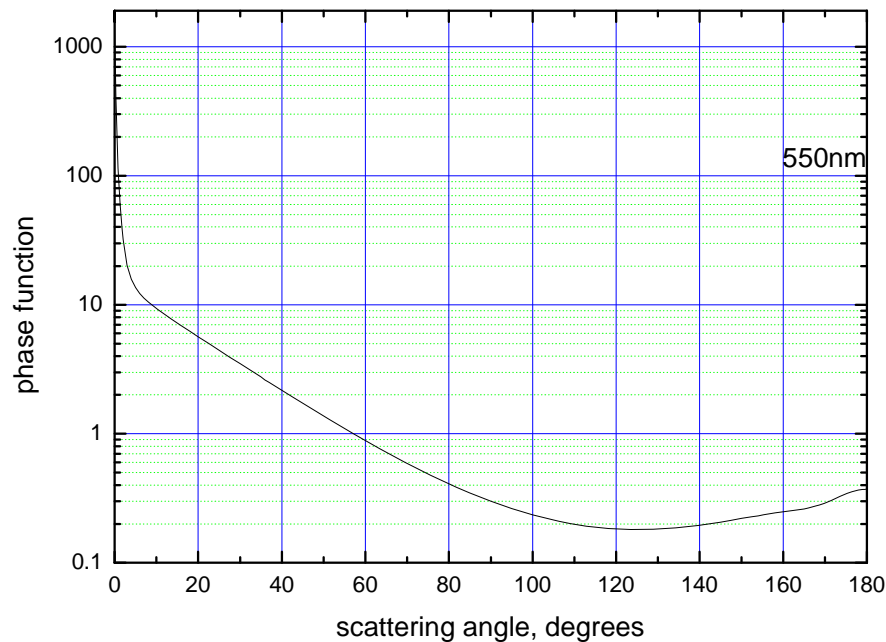
Fig. 1. The phase function used in retrievals.
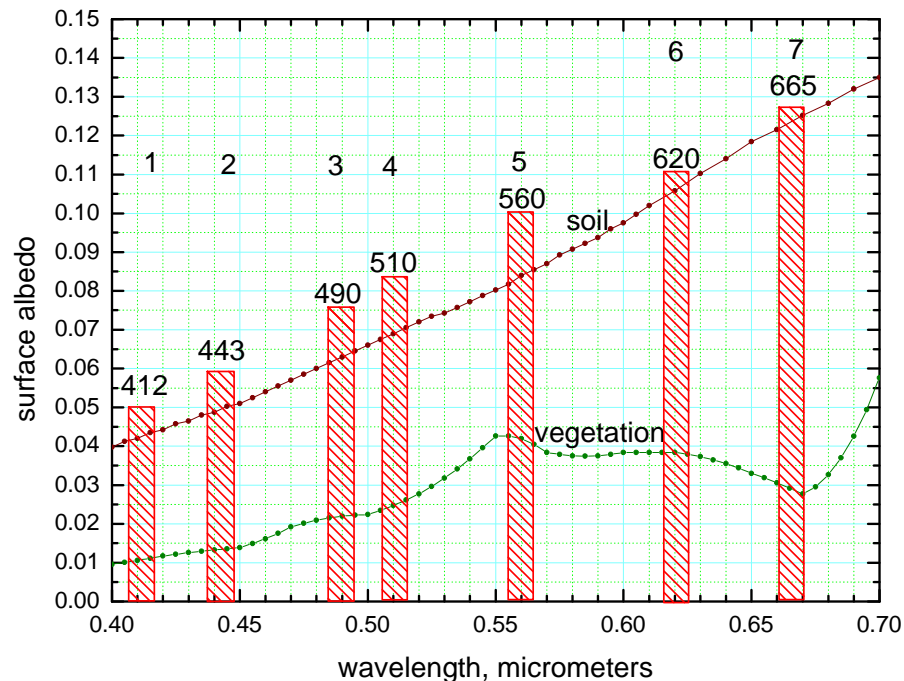
Fig. 2. The soil and vegetation spectral spherical albedos in the visible. MERIS channels 1–7 (in nm) are also shown. Spectra were obtained using airborne measurements (von Hoyningen-Huene et al., 2003).
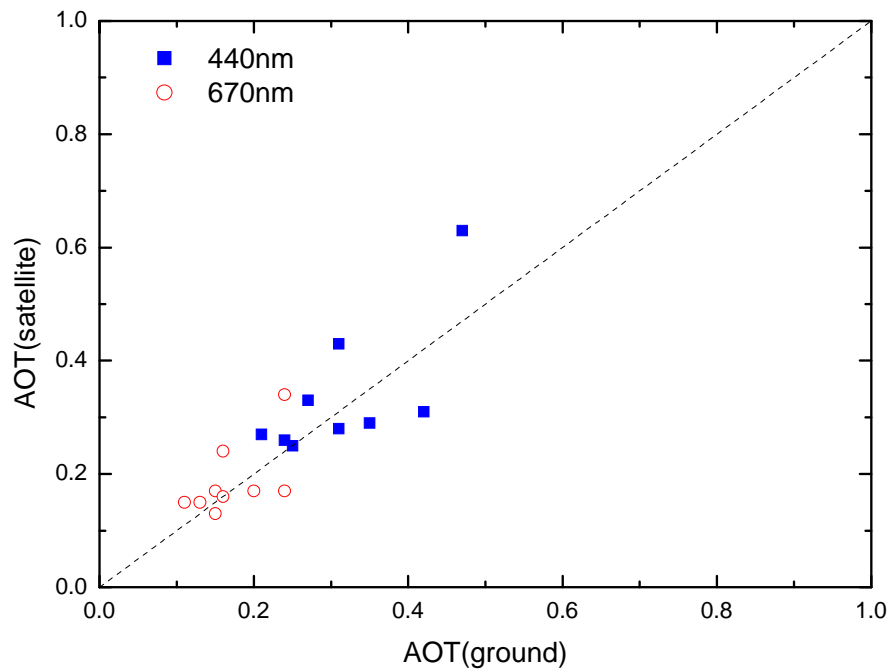
Fig. 3. The aerosol optical thickness correlation plot at the AERONET wavelengths 440 nm and 670 nm.
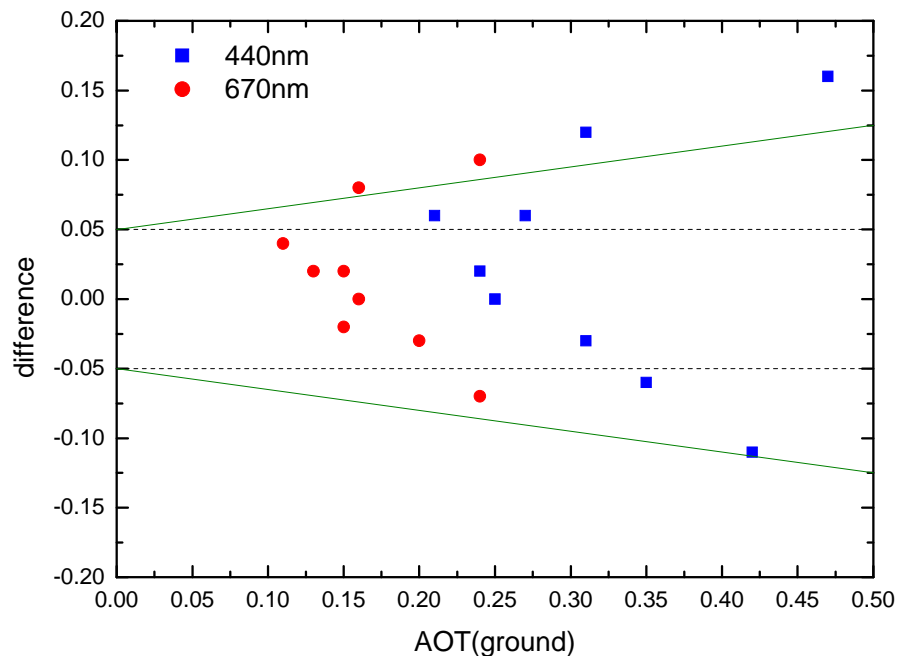
Fig. 4. The difference in AOTs derived from satellite and ground. The boundary errors (upper and lower lines) for the MODIS retrievals over land are also shown.
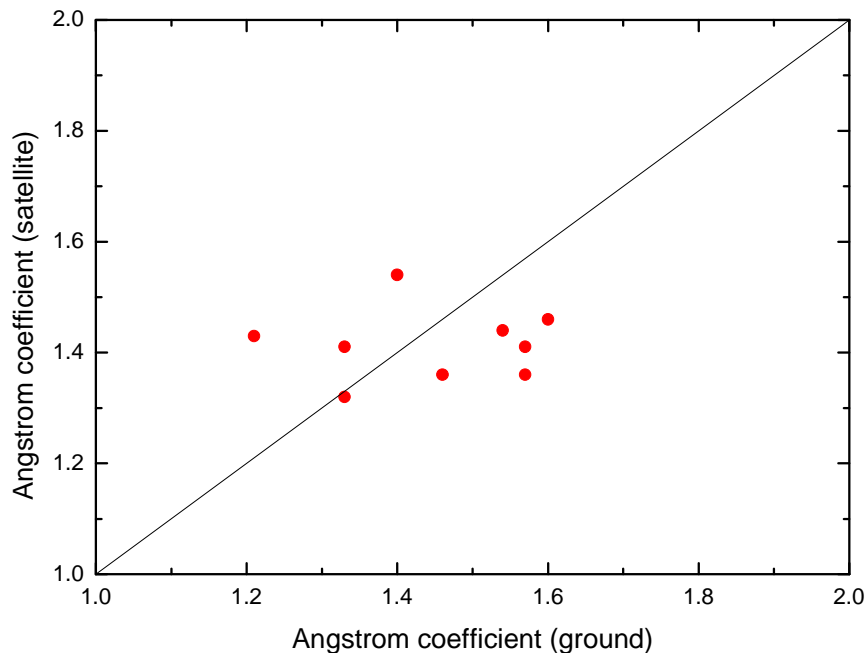
Fig. 5. The Angstrom parameter correlation plot. The Angstrom parameter was calculated at the AERONET wavelengths 440 nm and 670 nm.
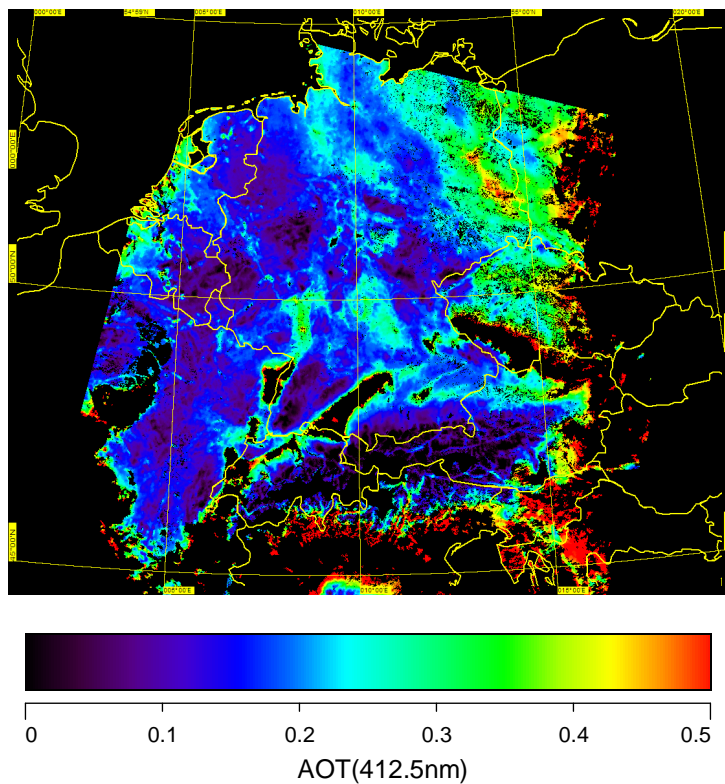
Fig. 6. The AOT spatial distribution at the wavelength 412.5 nm.
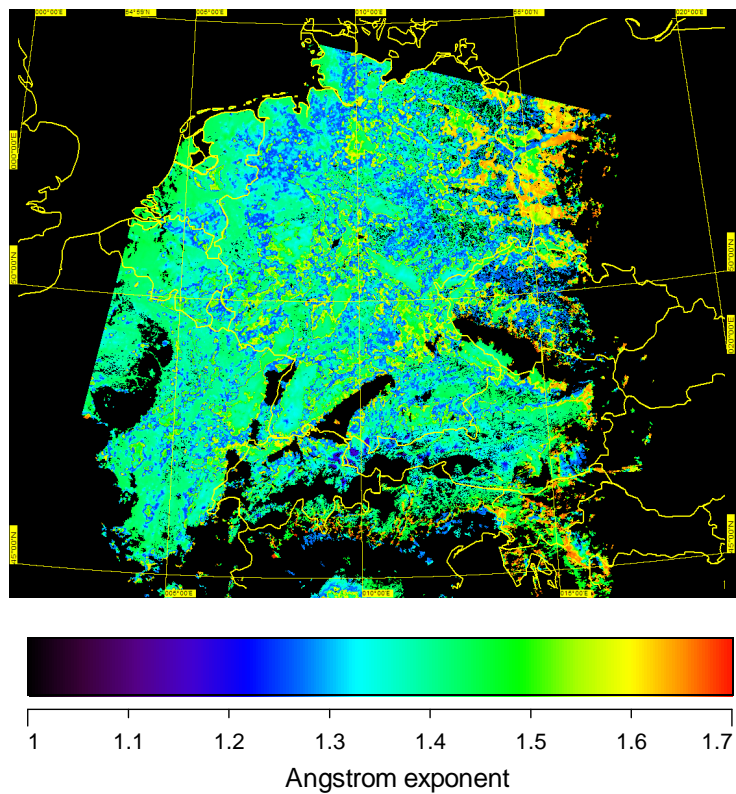
Fig. 7. The Angstrom exponent spatial distribution.

Title Page

Abstract | Introduction

Conclusions | References

Tables | Figures

◄ | ►

◄ | ►

Back | Close

Full Screen / Esc

Printer-friendly Version

Interactive Discussion
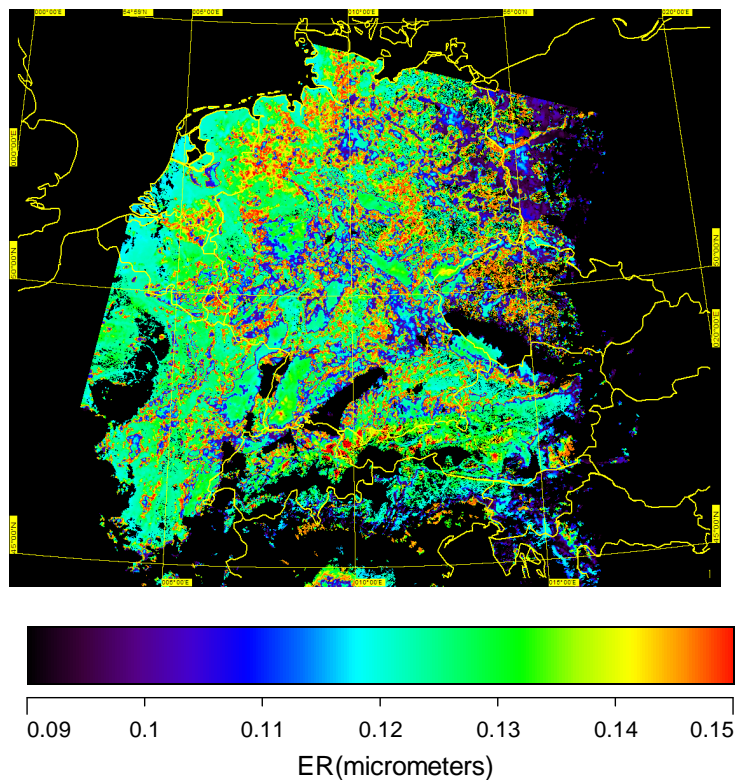
Fig. 8. The effective radius spatial distribution.
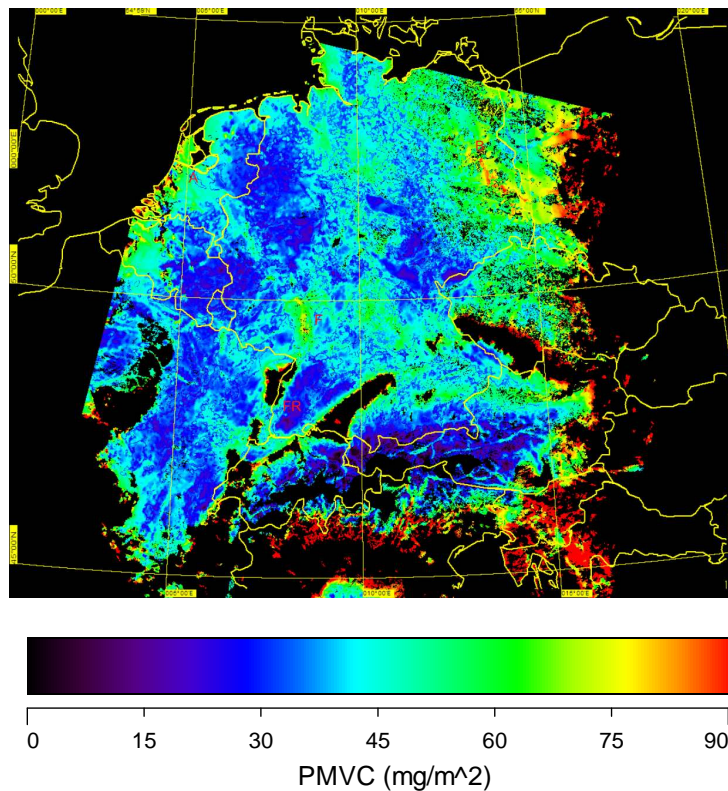
Fig. 9. The particulate matter vertical column map (A – Amsterdam, B – Berlin, F – Frankfurt, FR – Freiburg).
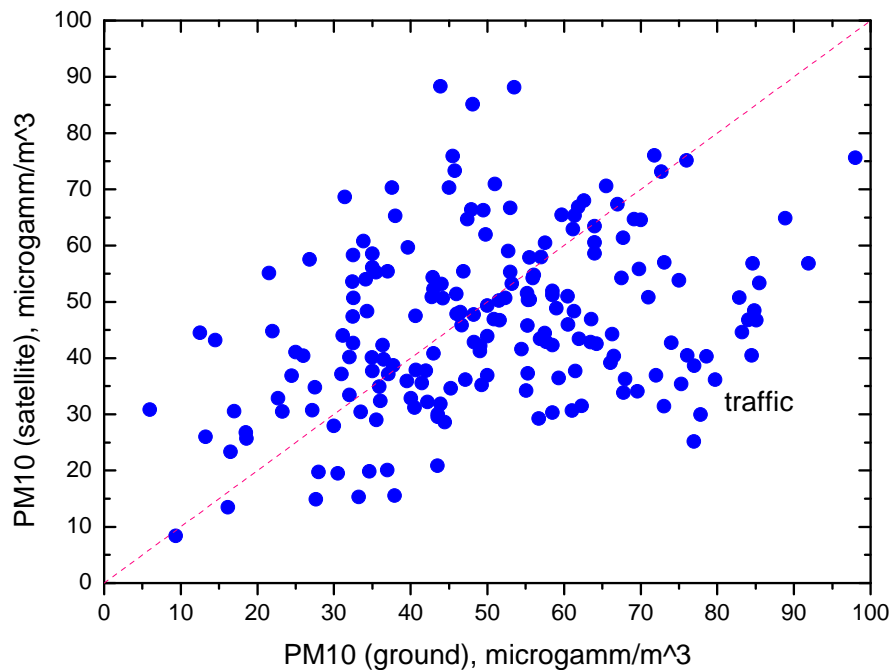
Fig. 10. The correlation plot for PM_{10} derived from ground and satellite measurements. The ECMWF boundary layer height information was used in the determination of PM_{10} (M=m/L).
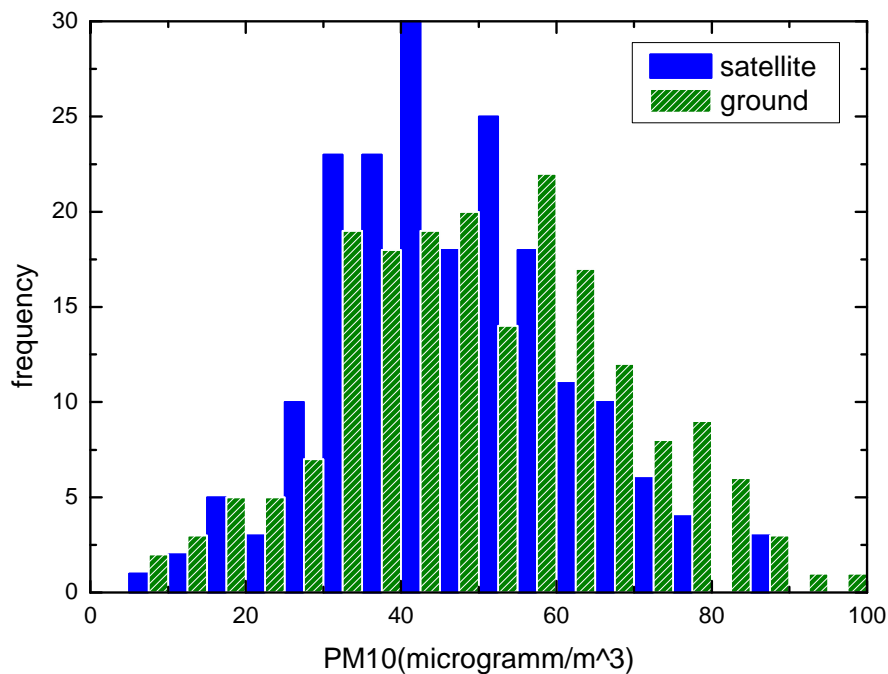
Fig. 11. The same as in Fig. 11 except in the form of a histogram.